https://doi.org/10.5194/bg-2020-177
Preprint. Discussion started: 3 July 2020


# Hysteretic temperature sensitivity of wetland $CH_4$ fluxes explained by substrate availability and microbial activity

Kuang-Yu Chang*,

Climate and Ecosystem Sciences Division, Lawrence Berkeley National Laboratory, Berkeley, California, USA

William J. Riley,

Climate and Ecosystem Sciences Division, Lawrence Berkeley National Laboratory, Berkeley, California, USA

Patrick M. Crill,

Department of Geological Sciences and Bolin Centre for Climate Research, Stockholm University, Stockholm, Sweden

Robert F. Grant,

Department of Renewable Resources, University of Alberta, Edmonton, Alberta, Canada

Scott R. Saleska

Department of Ecology and Evolutionary Biology, University of Arizona, Tucson, Arizona, USA

*Corresponding author: Kuang-Yu Chang, ckychang@lbl.gov

Climate and Ecosystem Sciences Division, Lawrence Berkeley National Laboratory

Berkeley, California, USA

Phone: (510) 495-8141

Key words: Methane cycling; microbial dynamics; climate change; IsoGenie Project; Stordalen Mire

https://doi.org/10.5194/bg-2020-177
Preprint. Discussion started: 3 July 2020

Biogeosciences Discussions
Open Access

**Abstract**

Methane ($CH_4$) emissions from wetlands are likely increasing and important in global climate change assessments. However, contemporary terrestrial biogeochemical model predictions of $CH_4$ emissions are very uncertain, at least in part due to prescribed temperature sensitivity of $CH_4$ production and emission. While statistically consistent apparent $CH_4$ emission temperature dependencies have been inferred from meta-analyses across microbial to ecosystem scales, year-round ecosystem-scale observations have contradicted that finding. Using flux observations and mechanistic modeling in two heavily studied high-latitude research sites (Stordalen, Sweden, and Utqiaġvik, Alaska, USA), we show here that substrate-mediated hysteretic microbial and abiotic interactions lead to intra-seasonally varying temperature sensitivity of $CH_4$ production and emission. We find that seasonally varying substrate availability drives lower and higher modeled methanogen biomass and activity, and thereby $CH_4$ production, during the earlier and later periods of the thawed season, respectively. Our findings demonstrate the uncertainty of inferring $CH_4$ emission or production from temperature alone, and highlight the need to represent microbial and abiotic interactions in wetland biogeochemical models.

https://doi.org/10.5194/bg-2020-177
Preprint. Discussion started: 3 July 2020


Biogeosciences Discussions

## 1. Introduction

Methane ($CH_4$) is the second most important climate forcing gas with at least a 28-fold higher global warming potential (GWP) than carbon dioxide ($CO_2$) over a 100-year horizon (Myhre, *et al* 2013). Atmospheric $CH_4$ concentrations have more than doubled since 1750 (Saunois et al., 2016) and have contributed about 20% of the additional radiative forcing accumulated in the lower atmosphere (Ciais et al., 2013). Recent assessments have found that $CH_4$ emissions from wetland and other inland waters are the largest and most uncertain sources affecting the global $CH_4$ budget (Kirschke et al., 2013; Poulter et al., 2017; Saunois et al., 2016). Such $CH_4$ emissions account for 25 to 32% of current global total $CH_4$ emissions (Saunois et al., 2016) and contribute substantially to the renewed and sustained atmospheric $CH_4$ growth after 2006 (Saunois et al., 2017). Increasing $CH_4$ emissions could offset mitigation efforts and accelerate climate change (Bastviken et al., 2011; Kirschke et al., 2013) due to their strong influence on the global radiative energy budget (Neubauer and Megonigal, 2015). However, $CH_4$ emission estimates are poorly constrained due to insufficient quality-controlled measurements (Bastviken et al., 2011; Kirschke et al., 2013; Saunois et al., 2016) and uncertain model structures and parameterizations (Melton et al., 2013; Wania et al., 2013; Xu et al., 2016). In fact, simulations in the ongoing Coupled Model Intercomparison Project Phase 6 (CMIP6; (Eyring et al., 2016)) do not even request wetland $CH_4$ emission predictions for the historical or 21$^{st}$ century periods. A number of knowledge gaps (Xu et al., 2016) need to be addressed to improve $CH_4$ model representations and thereby $CH_4$ climate feedback predictions (Dean et al., 2018). Such efforts are imperative because, among other reasons, permafrost degradation resulting from observed global-scale

https://doi.org/10.5194/bg-2020-177
Preprint. Discussion started: 3 July 2020

Biogeosciences Discussions
Open Access EGU

permafrost warming (Biskaborn et al., 2019) can stimulate organic matter decomposition (Schuur et al., 2015) that could augment global warming with a strong contribution from $CH_4$ (Knoblauch et al., 2018).

Many contemporary terrestrial biogeochemical models parameterize $CH_4$ production (or even $CH_4$ emissions) as a static temperature function of net primary production or heterotrophic respiration (Melton et al., 2013; Wania et al., 2013; Xu et al., 2016). Such parameterization is supported by recent meta-analyses that indicate a static and consistent apparent $CH_4$ production and emission temperature dependence across microbial to ecosystem scales (Yvon-Durocher et al., 2014). However, measurements collected across sites with nearly identical wetland climate, hydrology, and plant community compositions suggest large spatial and temporal variability in the ratio between ecosystem productivity and $CH_4$ emissions (Hemes et al., 2018). Further, ecosystem-scale $CH_4$ emissions have hysteretic responses to seasonal changes in gross primary productivity (GPP), water table depth (WTD), and temperature (Brown et al., 2014; Goodrich et al., 2015; Rinne et al., 2018; Zona et al., 2016), suggesting that $CH_4$ biogeochemistry may not be accurately represented by static relationships. Consequently, a mechanistic understanding of factors modulating $CH_4$ production and emission rates is urgently needed to improve the currently uncertain $CH_4$ biogeochemistry parameterization.

Here, we investigated the impacts of soil thermal and hydrological history on $CH_4$ emissions to improve understanding of apparent $CH_4$ emission temperature dependence and inform $CH_4$ model structure and parameterization. We hypothesized that a static apparent $CH_4$ emission temperature dependence is not sufficient for modeling

https://doi.org/10.5194/bg-2020-177
Preprint. Discussion started: 3 July 2020




$CH_4$ emissions due to substrate-mediated hysteretic microbial and abiotic interactions (Tang and Riley, 2014) over seasonal time scales. Specifically, we examined temperature responses of $CH_4$ emission and production rates measured and modeled in two heavily studied Arctic field sites (Metcalfe et al., 2018): the Stordalen Mire, Sweden (68.2 °N, 19.0 °E) and Utqiaġvik (formerly Barrow), Alaska (71.3 °N, 156.5 °W). We used a comprehensive biogeochemistry model (*eocsys*) to investigate the observed intra-seasonal changes in apparent $CH_4$ emission temperature dependence (e.g., Fig. 1) and evaluate the uncertainty of ignoring substrate-mediated hysteretic microbial and abiotic interactions. Although observations of increases in $CH_4$ emissions, spatial heterogeneity, and seasonal dynamics following permafrost degradation have been discussed (Hodgkins et al., 2014; McCalley et al., 2014; Olefeldt et al., 2013), an understanding of mechanisms regulating intra-seasonally varying $CH_4$ emissions and their response to temperature is still lacking.

## 2. Method

### 2.1 Study site description

The Stordalen Mire sites are about 10 km east of the Abisko Scientific Research Station in the discontinuous permafrost zone of northern Sweden and include intact permafrost palsa, partly thawed bog, and fen (Hodgkins et al., 2014). The mean annual air temperature and precipitation at the Stordalen Mire are around 0.6 °C and 336 mm $y^{-1}$, respectively. The measured $CH_4$ emissions are near zero in the palsa due to its deeper WTD and shallower Active Layer Depth (ALD) (Bäckstrand et al., 2008b, 2008a, 2010); we therefore did not include this site in our analysis. The bog is ombrotrophic (pH ~4.2) with WTD fluctuating from the peat surface to 35 cm below the peat surface (Bäckstrand et al., 2008b, 2008a; Olefeldt and Roulet, 2012), and is dominated by *Sphagnum* spp.

https://doi.org/10.5194/bg-2020-177
Preprint. Discussion started: 3 July 2020


Biogeosciences Discussions
Open Access

mosses with a moderate abundance of short sedges such as *Eriophorum vaginatum* and *Carex bigelowii* (Bäckstrand et al., 2008b, 2008a; Malmer et al., 2005; Olefeldt and Roulet, 2012). The fen is minerotrophic (pH~5.7), has WTD near or above the peat surface throughout the growing season, and is dominated by tall sedges such as *E. angustifolium*, *C. rostrata* and *Esquisetum* spp. (Bäckstrand et al., 2008b, 2008a; Olefeldt and Roulet, 2012). The Stordalen Mire bog and fen both have a peat layer ranging from 0.5 to 1 m (Rydén and Kostov, 1980) and an ALD greater than 0.9 m (Bäckstrand et al., 2008b).

The Utqiaġvik site is located at the Barrow Experimental Observatory at the northern tip of Alaska's Arctic coastal plain, which is characterized by polygonal landforms caused by seasonal freezing and thawing of tundra soil (Hinkel et al., 2005). These polygonal landforms were categorized into separate features based on moisture variation determined by surface elevations (Wainwright et al., 2015). We analyzed $CH_4$ emissions modeled in the low-centered polygonal landform that was represented as a connected combination of trough, rim, and center structures (Grant et al., 2017b). The mean annual air temperature and precipitation at Utqiaġvik are around -12°C and 106 mm $y^{-1}$, respectively. The ALD varies spatially from approximately 20 to 60 cm, which is influenced by soil texture, vegetation, soil moisture, and inter-annual variability (Shiklomanov et al., 2010).

## 2.2 Field measurements

A system of six automated gas-sampling chambers made of transparent Lexan was installed at the Stordalen Mire in 2001 (three in the bog and three in the fen). Each chamber covered an area of 0.14 $m^2$ (38 cm × 38 cm) with a height of 25–45 cm

https://doi.org/10.5194/bg-2020-177
Preprint. Discussion started: 3 July 2020




depending on the vegetation and the depth of insertion, and was closed for 5 minutes every 3 hours. In addition, each chamber is instrumented with thermocouples measuring air and ground surface temperatures, and WTD is measured manually three to five times per week from June to October each year (McCalley et al., 2014). The system was updated with a new chamber design similar to that described in (Bubier et al., 2003) in 2011. The new chambers each cover an area of 0.2 m$^2$ (45 cm × 45 cm), with a height ranging from 15 to 75 cm depending on habitat vegetation. We analyze time- and chamber- specific daily mean $CH_4$ emissions and ground temperature (when there are at least six 3-hourly measurements per day) recorded in the Stordalen Mire during the thawed seasons to identify the observed apparent $CH_4$ emission temperature dependence. We cannot infer an apparent $CH_4$ emission temperature dependence that only recognizes temperature effects at the Utqiaġvik site because continuous landform specific (i.e., trough-, rim-, and center- specific) measurements are not available there.

### 2.3 Apparent temperature dependence calculation

We quantify the apparent temperature dependencies of daily $CH_4$ emission and $CH_4$ production by fitting Boltzmann-Arrhenius functions of the form:

$$\ln F_i(T) = \overline{E_{a,i}} \cdot \left(\frac{-1}{kT}\right) + \varepsilon_{F_i} \qquad \text{(Eq. 1)}$$

where $F_i(T)$ is the rate of $CH_4$ emission (i = 1) and $CH_4$ production (i = 2) at absolute temperature T. $\overline{E_{a,i}}$ (in eV) and $\varepsilon_{F_i}$ correspond to the fitted apparent activation energy (slope) and base reaction rate (intercept), respectively. $k$ is the Boltzmann constant ($8.62 \times 10^{-5}$ eV K$^{-1}$).

We defined earlier and later periods as the time before and after the modeled (or measured) temperature (air or soil) reaching its maximum value in a thawed season,

https://doi.org/10.5194/bg-2020-177
Preprint. Discussion started: 3 July 2020


respectively, to investigate intra-seasonal changes in apparent $CH_4$ emission or production temperature dependencies. Thawed seasons were defined as the time period when modeled vertical mean 0-20 cm soil temperatures (or measured air and ground surface temperatures) are at least 1 °C to avoid low $CH_4$ emissions in the 0 – 1 °C temperature window that can alter the base reaction rate of our Boltzmann-Arrhenius functions. The vertical mean 0 – 20 cm soil temperature was chosen for our analysis because $CH_4$ production in our study site is concentrated in the top 20 cm of soil (Chang et al., 2019b). Consistent hysteretic temperature responses were derived with above zero vertical mean 0 – 20 cm soil temperatures (i.e., include the 0 – 1 °C temperature window), e.g., Fig. 2 vs. Supplementary Fig. 1.

**2.4 Model description**

The *ecosys* model is a comprehensive biogeochemistry model that explicitly represents interactions among biogeophysical (i.e., hydrological and thermal), biogeochemical (including carbon, nitrogen, and phosphorus), plant and microbial processes. The above-ground processes are represented in multi-specific multi-layer plant canopies, and the below-ground processes are represented in multiple soil layers with multiphase subsurface reactive transport. $CH_4$ production (i.e., acetoclastic and hydrogenotrophic methanogenesis), $CH_4$ oxidation, and $CH_4$ transport (i.e., diffusion, aerenchyma, and ebullition) are explicitly represented in *ecosys*. The *ecosys* model operates at variable time steps (~seconds to 1 hour) determined by convergence criteria, and it can be applied at patch scale (spatially homogenous one-dimensional; e.g., (Chang et al., 2019a)) and landscape scale (spatially variable two- or three-dimensional; e.g., (Grant et al., 2017b, 2017a)). The *ecosys* model has been extensively examined against field measurements made in 2002–2007 (Chang et al., 2019a) and 2011–2013 (Chang et al., 2019b) in our study sites at the Stordalen Mire, and 2013 in our study sites at Utqiagvik (Grant et al., 2017b, 2017a, 2019). A qualitative summary of the *ecosys* model is provided in the supplementary material to this article, and detailed descriptions are available in the supplements of (Grant et al., 2017b, 2017a). The *ecosys* model structure remains unchanged from that in earlier studies.

**2.5 Experimental design**

The primary purpose of this study is to explore the implications of the observed $CH_4$ emission hysteresis (Fig. 1) and highlight the need to recognize factors other than temperature that control ecosystem-scale $CH_4$ emissions. We develop a mechanistic explanation for such hysteresis by investigating how the modeled environmental drivers modulate $CH_4$ emission hysteresis. The modeled data used in this study are extracted from our earlier simulations that can be downloaded from the IsoGenie database (https://isogenie-db.asc.ohio-state.edu/; (Chang et al., 2019a, 2019b)) and the NGEE-Arctic database (https://ngee-arctic.ornl.gov/; (Grant et al., 2017b, 2017a)). Our analysis focuses on modeled data because some factors (e.g., root exudates, substrate availability, and methanogenic population and activity) modulating $CH_4$ production and emission rates are not continuously measured at our study sites. Our recently published model results at the Stordalen Mire and Utqiaġvik sites indicate good comparisons with observations, including for thaw depth ($R^2$ = 0.75 to 0.90), WTD (mean bias = -4.3 to 4.0 cm), and $CO_2$ ($R^2$ = 0.43 to 0.88) and $CH_4$ ($R^2$ = 0.31 to 0.93) surface fluxes (Chang et al., 2019a, 2019b; Grant et al., 2017b, 2017a, 2019). For conciseness, we focus discussion in the remainder of the paper on the Stordalen Mire fen site, since it exhibits strong apparent

https://doi.org/10.5194/bg-2020-177
Preprint. Discussion started: 3 July 2020


hysteresis and the underlying mechanisms leading to hysteretic $CH_4$ emissions are similar across all study sites.

We note the relevant point that the *ecosys* model itself represents temperature dependence of soil metabolic activity and gas production through locally simulated soil temperature profiles with an modified Arrhenius function that includes terms for low- and high-temperature inactivation (Grant, 2015). Besides temperature effects, the *ecosys* model also represents substrate controls (through Michaelis-Menten kinetics) on microbial biomass and activity (e.g., Chang et al., 2019b), which is not explicitly characterized by inferring an apparent whole system temperature dependence (e.g., Eq. 1). These representations allow the model to simulate overall $CH_4$ emission patterns with more complex dynamics than represented in the apparent temperature dependence function alone, making it a suitable tool for investigating the relative importance of temperature dependence versus other factors.

## 3. Results and discussion

### 3.1 Observed patterns of apparent $CH_4$ emission hysteresis

The $CH_4$ emissions measured in the Stordalen Mire bog and fen exhibit hysteretic responses to ground surface temperature: i.e., at the same ground surface temperature, greater $CH_4$ emissions during the later than the earlier periods of the thawed season (Fig. 1). At both sites, plotting time- and chamber- specific $CH_4$ emission and ground surface temperature measurements from the beginning to end of the thawed season results in a counterclockwise hysteresis loop at each site-year (2012 to 2017). Such hysteretic responses lead to intra-seasonally varying apparent $CH_4$ emission temperature dependencies, suggesting that recognizing temporal variability is needed to

https://doi.org/10.5194/bg-2020-177
Preprint. Discussion started: 3 July 2020




quantify factors modulating $CH_4$ emissions. For example, three distinct apparent $CH_4$ emission temperature dependencies can be derived from the same chamber sampling at different periods within the same thawed season (i.e., earlier period, later period, and full season). Despite the high spatial heterogeneity, the observed patterns of $CH_4$ emission hysteresis are consistent between chambers within and between the bog and fen habitats. Our results thus demonstrate that $CH_4$ emissions are generally more sensitive to temperature changes during the later part of the thawed season, and that $CH_4$ emission strength and temperature dependence vary substantially among site-years. Consistent hysteretic responses can be found in $CH_4$ emission and air temperature measurements (Supplementary Fig. 2) and in measurements collected from 2003 to 2008 with relatively sparse data records (Supplementary Fig. 3). Ignoring the large spatial and temporal variability in apparent $CH_4$ emission temperature dependencies may not accurately represent the underlying dynamics, even though the inferred apparent activation energy for $CH_4$ emissions is comparable between the habitats (e.g., Supplementary Fig. 4).

### 3.2 Modeled patterns of apparent $CH_4$ emission hysteresis

The $CH_4$ emissions modeled by *ecosys*, extracted from our recently published results in the Stordalen Mire and the Utqiaġvik sites (Chang et al., 2019b; Grant et al., 2017b), have hysteretic responses to mean 0–20 cm soil temperature (Fig. 2) and air temperature (Supplementary Fig. 5). The apparent $CH_4$ emission temperature dependence inferred from the modeled results varies substantially from the beginning to the end of the thawed season, suggesting that $CH_4$ emissions may not be accurately represented as a single function of temperature. For each site-year, $CH_4$ emissions modeled in the later period are greater than those in the earlier period at the same temperature (e.g., Fig. 2),

https://doi.org/10.5194/bg-2020-177
Preprint. Discussion started: 3 July 2020



consistent with observations (e.g., Fig. 1). The apparent hysteresis is larger and clearer in the Stordalen Mire fen compared to the bog and the Utqiaġvik low-centered polygon, likely from its warmer soil temperatures, shallower WTD, and higher $CH_4$ emissions (Chang et al., 2019b). In addition to temporal variability, changes in biogeophysical conditions driven by fine-scale hydrology and vegetation differences can also alter the apparent functional relationship between $CH_4$ emission and temperature. For example, apparent $CH_4$ emission temperature dependencies inferred for individual topographic features (i.e., troughs, rims, and centers) vary substantially within the same wetland ecosystem at Utqiaġvik (Supplementary Fig. 6), despite being driven by the same meteorological forcing.

We evaluate the effects of intra-seasonal variability on ecosystem-scale $CH_4$ emissions by estimating apparent $CH_4$ emission temperature dependencies during different parts of the thawed season. By fitting the Boltzmann-Arrhenius function (Eq. 1) to the $CH_4$ emissions and 0–20 cm soil temperatures modeled during different time frames (i.e., earlier period, later period, and full season), we developed and evaluated three temperature dependence models for each thawed season. Our results show that $CH_4$ emission estimates improve when apparent $CH_4$ emission temperature dependencies were separately represented in the earlier and later periods, compared to those assuming a seasonally invariant apparent $CH_4$ emission temperature dependence (Supplementary Table 1, 2). In the Stordalen Mire, neglecting intra-seasonal variability in apparent $CH_4$ emission temperature dependence leads to overestimated (10 to 81%) and underestimated (-21 to -40%) $CH_4$ emissions during the earlier and later periods, respectively (Supplementary Table 1). Consistent prediction bias was found in the Utqiaġvik low-centered polygon, except in the rims where drier conditions limit $CH_4$ emissions (Supplementary Table 2).

These results demonstrate that models based on a seasonally invariant apparent $CH_4$ emission temperature dependence may introduce errors by improperly prescribing the seasonal dynamics of $CH_4$ biogeochemistry with a static function of temperature. The substantial intra-seasonal variability, potentially led by site specific thermal and hydrological history (Updegraff et al., 1998), could be an important and overlooked property of natural wetlands that currently account for 25 to 32% of global total $CH_4$ emissions (Saunois et al., 2016). Representing intra-seasonally variable apparent $CH_4$ emission or production temperature dependencies in large-scale wetland biogeochemical models may thus reduce $CH_4$ emission prediction biases and model structural uncertainty.

### 3.3 Microbial substrate-mediated $CH_4$ production hysteresis

For conciseness, we focus our discussion on the potential drivers causing the hysteretic relationship between $CH_4$ emission and soil temperature modeled in the Stordalen Mire fen site at 2011, as the underlying mechanisms are consistent across all site-years. The temporal evolution of $CH_4$ emissions modeled by *ecosys* follows that of $CH_4$ production (Fig. 3a), with less than 5% of the modeled $CH_4$ production offset by $CH_4$ oxidation in the Stordalen Mire sites during the thawed season (Chang et al., 2019b). Modeled $CH_4$ emission (e.g., Fig. 2d) and production (Fig. 3b) rates both exhibit intra-seasonal variations in their apparent temperature dependencies during the thawed season, consistent with the varying temperature responses to microbial thermal history reported in laboratory incubations (Updegraff et al., 1998). The relatively low $CH_4$ oxidation suggests that hysteretic responses of modeled $CH_4$ emissions to temperature (Fig. 2)

https://doi.org/10.5194/bg-2020-177
Preprint. Discussion started: 3 July 2020



primarily result from hysteretic $CH_4$ production (Fig. 3b) associated with asymmetric methanogen biomass (Fig. 3c) and activity (Fig. 3d) between the earlier and later periods. This result is consistent with isotopic measurements which also indicated that changes in $CH_4$ production, not $CH_4$ oxidation, determine the $CH_4$ emissions observed in the Stordalen Mire sites (Hodgkins et al., 2014; McCalley et al., 2014).

Increased soil temperatures elevate oxygen demands for aerobic heterotrophs while reducing oxygen solubility, which favors fermenter and methanogens and thereby enhance $CH_4$ production. Our model results indicate that the elevated methanogen biomass and activity during the later period are driven by the increased substrate availability for methanogenesis later in the thawed season. Modeled substrate concentrations remain relatively high after peak substrate production rate at maximum seasonal soil temperature for both acetoclastic (AM; Fig. 4a) and hydrogenotrophic methanogenesis (HM; Fig. 5a). Relatively high AM (Fig. 4b) and HM (Fig. 5b) substrate availability during the later period elevates AM and HM energy yields at a given soil temperature, resulting in higher methanogen growth (Fig. 3d) and biomass (Fig. 3c) later in the thawed season. Therefore, $CH_4$ production rates during the later period become higher than those during the earlier period at the same soil temperature (Fig. 3b), which drives higher $CH_4$ emissions with increased aqueous $CH_4$ concentrations. Although AM and HM each exhibit microbial substrate-mediated hysteretic temperature responses, AM appears to be more hysteretic to soil temperature than HM (Fig. 6). The stronger AM hysteresis is consistent with the larger and clearer $CH_4$ emission hysteresis found in the Stordalen Mire fen (Fig. 2), where the fractional contribution of AM to total $CH_4$ production is higher than in the Stordalen Mire bog (Chang et al., 2019b; McCalley et al.,

https://doi.org/10.5194/bg-2020-177
Preprint. Discussion started: 3 July 2020



2014). A schematic summarizing the above-mentioned mechanisms for microbial substrate-mediated $CH_4$ production hysteresis is presented in Fig. 7.

**3.4 Other factors regulating intra-seasonal $CH_4$ emissions**

To evaluate whether our finding that microbial substrate-mediated $CH_4$ production is the primary cause of the observed hysteresis with temperature, we evaluated four alternative hypotheses: interactions with (1) water table depth; (2) GPP (via exudation, root litter inputs, and aerenchyma development); (3) thaw depth; and (4) residual pore-water $CH_4$ concentrations at the end of the earlier part of the thawed season.

First, studies have found that seasonal variations of WTD determine $CH_4$ cycling dynamics by regulating the temperature response of $CH_4$ emissions, leading to the observed $CH_4$ emission hysteresis when drought-induced WTD drawdown below the critical zone for $CH_4$ production (Brown et al., 2014; Goodrich et al., 2015). The substantial $CH_4$ emission hysteresis observed at the Stordalen Mire fen site is unlikely caused by seasonal variations in WTD, because the observed WTD are around or above the peat surface throughout the thawed season with limited effects on $CH_4$ emissions (Bäckstrand et al., 2008b).

Second, Rinne et al. (2018) reported that the temporal variations of $CH_4$ emissions are strongly regulated by GPP, and the time required to convert GPP to methanogenesis substrates may cause the observed apparent hysteresis found between GPP and $CH_4$ emissions. Our results show apparent hysteresis between GPP and $CH_4$ emissions modeled at our study sites (e.g., Fig. 8a), suggesting higher $CH_4$ emissions later in the thawed season at a given GPP. We next analyzed these interactions using *ecosys* at the Stordalen Mire fen site to explore whether an apparent hysteretic

https://doi.org/10.5194/bg-2020-177
Preprint. Discussion started: 3 July 2020




relationship between $CH_4$ emissions and GPP is causally connected. We examined three primary pathways by which GPP could lead to a delayed effect on $CH_4$ emissions, and thereby hysteresis: increases in (1) fresh carbon inputs from root exudation (Fig. 8b), (2) below-ground litter inputs (Fig. 8c), and (3) aerenchyma transport caused by GPP-induced growth of porous sedge roots (Fig. 8d). In contrast to the apparent hysteresis with GPP, all three of these mechanisms exhibit reversed hysteresis cycles compared to those between $CH_4$ emissions and temperature. Therefore, these three primary mechanisms are inconsistent with a causal hysteretic relationship between GPP and $CH_4$ emissions.

Third, studies have suggested that soil temperature increases can expand the volume of unfrozen soil and thereby stimulate deep carbon decomposition, which can also contribute to higher carbon emissions later in the thawed season, as has been observed for upland $CO_2$ emissions (Goulden et al., 1998) and wetland $CH_4$ emissions (Iwata et al., 2015). Our results show a weak correlation between thaw depth and $CH_4$ emissions during the latter part of the thawed season, although $CH_4$ emissions appear to increase with deeper thaw during the earlier period (Fig. 8e). Therefore, the hysteretic relationship between $CH_4$ emission and soil temperature found in our study sites is not causally connected with the greater volume of unfrozen soil later in the thawed season. This may be explained by the relatively shallow zone (mostly within the top 20 cm of soil) of $CH_4$ production (Chang et al., 2019b) compared with the much deeper thaw depth modeled during the peak $CH_4$ emission period (i.e., July to August) (Chang et al., 2019a).

Fourth, we conducted a sensitivity test, by forcing zero $CH_4$ production during the later period, to examine the amount of lagged $CH_4$ emissions resulting from $CH_4$ residual stored in the soil profile at the end of the earlier part of the thawed season that

https://doi.org/10.5194/bg-2020-177
Preprint. Discussion started: 3 July 2020


Biogeosciences Discussions Open Access EGU

contributes to apparent $CH_4$ emission hysteresis. At the Stordalen Mire fen, later-period $CH_4$ emissions resulting from earlier-period $CH_4$ residual concentrations decreased approximately exponentially and contributed about 25% of the $CH_4$ emissions during the later period (Fig. 9). The timing and magnitude of later-period $CH_4$ emissions attributed to lagged $CH_4$ emissions do not match with the relatively high $CH_4$ emissions modeled during the later period. Therefore, our results suggest that lagged $CH_4$ emissions from residual $CH_4$ produced in the earlier period contribute to, but are not a dominant factor, modulating the apparent $CH_4$ emission hysteresis.

Collectively, our results suggest that microbial substrate-mediated $CH_4$ production hysteresis is the primary control of the observed apparent $CH_4$ emission hysteresis. The physical controls on $CH_4$ production and emission (and potentially their hysteresis patterns) in the sediments of terrestrial freshwater systems may differ from those we derived from vegetated peat surfaces (Wik et al., 2016), and further investigation is needed to assess their apparent temperature dependence. To better understand factors controlling $CH_4$ production and emission, continuous measurements of seasonal development of methanogenesis substrates and soil temperature at the depth where $CH_4$ production is prevalent are needed.

## 4. Conclusions

Many contemporary $CH_4$ models parameterize wetland $CH_4$ production (or emission) as a fixed fraction of net primary productivity or heterotrophic respiration regulated by a single static function of temperature (Melton et al., 2013; Wania et al., 2013). Our results suggest that such a parameterization is not accurate because it oversimplifies microbial responses to changing thermal and hydrological conditions that modulate wetland $CH_4$ production and emission rates. More continuous observations across sites are required to assess model prediction uncertainty and the broader extent to which our mechanistic explanations apply. In summary, we found that apparent $CH_4$ emission temperature dependencies vary from the earlier to later part of the thawed season due to substrate-mediated $CH_4$ production hysteresis caused by intra-seasonal changes in methanogen biomass and activity. We examined four alternative mechanisms that may contribute to the observed $CH_4$ emission hysteresis with temperature, and found none of them can exclusively explain the underlying dynamics. Our findings motivate explicit model representations of microbial dynamics that physiologically link microbial and abiotic interactions, as only three of 40 recently reviewed $CH_4$ models mechanistically represent $CH_4$ biogeochemistry (Xu et al., 2016).

## Acknowledgements

This study was funded by the Genomic Science Program of the United States Department of Energy Office of Biological and Environmental Research under the ISOGENIE (DE-SC0016440) and NGEE-Arctic projects under contract DE-AC02-05CH11231 to Lawrence Berkeley National Laboratory and grants from Swedish VR (Vetenskaprådet) and Swedish FORMAS to PMC. We acknowledge US National Science Foundation MacroSystems program (NSF EF 1241037) support for autochamber measurements between 2013 and 2017. We thank the Abisko Scientific Research Station of the Swedish Polar Research Secretariat for providing the meteorological data. The data presented in this study are available at the NGEE Arctic Database (doi:10.5440/1635534). The *ecosys* source code is available at Zenodo (doi:10.5281/zenodo.3906642).

https://doi.org/10.5194/bg-2020-177
Preprint. Discussion started: 3 July 2020


## References

Bäckstrand, K., Crill, P. M., Mastepanov, M., Christensen, T. R. and Bastviken, D.: Non-methane volatile organic compound flux from a subarctic mire in Northern Sweden, Tellus, Ser. B Chem. Phys. Meteorol., doi:10.1111/j.1600-0889.2007.00331.x, 2008a.

Bäckstrand, K., Crill, P. M., Mastepanov, M., Christensen, T. R. and Bastviken, D.: Total hydrocarbon flux dynamics at a subarctic mire in northern Sweden, J. Geophys. Res. Biogeosciences, doi:10.1029/2008JG000703, 2008b.

Bäckstrand, K., Crill, P. M., Jackowicz-Korczyñski, M., Mastepanov, M., Christensen, T. R. and Bastviken, D.: Annual carbon gas budget for a subarctic peatland, Northern Sweden, Biogeosciences, 7(1), 95–108, doi:10.5194/bg-7-95-2010, 2010.

Bastviken, D., Tranvik, L. J., Downing, J. A., Crill, P. M. and Enrich-Prast, A.: Freshwater methane emissions offset the continental carbon sink, Science (80-. )., 331(6013), 50, doi:10.1126/science.1196808, 2011.

Biskaborn, B. K., Smith, S. L., Noetzli, J., Matthes, H., Vieira, G., Streletskiy, D. A., Schoeneich, P., Romanovsky, V. E., Lewkowicz, A. G., Abramov, A., Allard, M., Boike, J., Cable, W. L., Christiansen, H. H., Delaloye, R., Diekmann, B., Drozdov, D., Etzelmüller, B., Grosse, G., Guglielmin, M., Ingeman-Nielsen, T., Isaksen, K., Ishikawa, M., Johansson, M., Johannsson, H., Joo, A., Kaverin, D., Kholodov, A., Konstantinov, P., Kröger, T., Lambiel, C., Lanckman, J. P., Luo, D., Malkova, G., Meiklejohn, I., Moskalenko, N., Oliva, M., Phillips, M., Ramos, M., Sannel, A. B. K., Sergeev, D., Seybold, C., Skryabin, P., Vasiliev, A., Wu, Q., Yoshikawa, K., Zheleznyak, M. and Lantuit, H.: Permafrost is warming at a global scale, Nat. Commun., 10(1), 1–11, doi:10.1038/s41467-018-08240-4, 2019.

https://doi.org/10.5194/bg-2020-177
Preprint. Discussion started: 3 July 2020

Biogeosciences Discussions Open Access EGU

Brown, M. G., Humphreys, E. R., Moore, T. R., Roulet, N. T. and Lafleur, P. M.: Evidence for a nonmonotonic relationship between ecosystem-scale peatland methane emissions and water table depth, J. Geophys. Res. Biogeosciences, 119(5), 826–835, doi:10.1002/2013JG002576, 2014.

Bubier, J., Crill, P., Mosedale, A., Frolking, S. and Linder, E.: Peatland responses to varying interannual moisture conditions as measured by automatic $CO_2$ chambers , Global Biogeochem. Cycles, doi:10.1029/2002gb001946, 2003.

Chang, K.-Y. and Riley, W.: Hysteretic temperature sensitivity of wetland CH4 fluxes explained by substrate availability and microbial activity: Model Archive, Next Gener. Ecosyst. Exp. Arct. Data Collect. Oak Ridge Natl. Lab. U.S. Dep. Energy, Oak Ridge, Tennessee, USA, doi:10.5440/1635534, 2020.

Chang, K.-Y., Riley, W. J., Crill, P. M., Grant, R. F., Rich, V. I. and Saleska, S. R.: Large carbon cycle sensitivities to climate across a permafrost thaw gradient in subarctic Sweden, Cryosph., 13(2), 647–663, doi:10.5194/tc-13-647-2019, 2019a.

Chang, K.-Y., Riley, W. J., Brodie, E. L., McCalley, C. K., Crill, P. M. and Grant, R. F.: Methane Production Pathway Regulated Proximally by Substrate Availability and Distally by Temperature in a High-Latitude Mire Complex, J. Geophys. Res. Biogeosciences, 2019JG005355, doi:10.1029/2019JG005355, 2019b.

Ciais, P., Sabine, C., Bala, G., Bopp, L., Brovkin, V., Canadell, J., Chhabra, A., DeFries, R., Galloway, J., Heimann, M., Jones, C., Quéré, C. Le, Myneni, R. B., Piao, S. and Thornton, P.: Carbon and Other Biogeochemical Cycles, in Climate Change 2013 - The Physical Science Basis, edited by Stocker, T.F., D. Qin, G.-K. Plattner, M. Tignor, S. K. Allen, J. Boschung, A. Nauels, Y. Xia, V. Bex, and P. M. Midgley, pp. 465–570, Cambridge

https://doi.org/10.5194/bg-2020-177
Preprint. Discussion started: 3 July 2020



University Press, Cambridge, United Kingdom and New York, NY, USA, Cambridge., 2013.

Dean, J. F., Middelburg, J. J., Röckmann, T., Aerts, R., Blauw, L. G., Egger, M., Jetten, M. S. M., de Jong, A. E. E., Meisel, O. H., Rasigraf, O., Slomp, C. P., in't Zandt, M. H. and Dolman, A. J.: Methane Feedbacks to the Global Climate System in a Warmer World, Rev. Geophys., 56(1), 207–250, doi:10.1002/2017RG000559, 2018.

Eyring, V., Bony, S., Meehl, G. A., Senior, C. A., Stevens, B., Stouffer, R. J. and Taylor, K. E.: Overview of the Coupled Model Intercomparison Project Phase 6 (CMIP6) experimental design and organization, Geosci. Model Dev., 9(5), 1937–1958, doi:10.5194/gmd-9-1937-2016, 2016.

Goodrich, J. P., Campbell, D. I., Roulet, N. T., Clearwater, M. J. and Schipper, L. A.: Overriding control of methane flux temporal variability by water table dynamics in a Southern Hemisphere, raised bog, J. Geophys. Res. Biogeosciences, 120(5), 819–831, doi:10.1002/2014JG002844, 2015.

Goulden, M. L., Wofsy, S. C., Harden, J. W., Trumbore, S. E., Crill, P. M., Gower, S. T., Fries, T., Daube, B. C., Fan, S.-M., Sutton, D. J., Bazzaz, A. and Munger, J. W.: Sensitivity of Boreal Forest Carbon Balance to Soil Thaw, Science (80-. )., 279(5348), 214–217, doi:10.1126/science.279.5348.214, 1998.

Grant, R. F.: Ecosystem CO2 and CH4 exchange in a mixed tundra and a fen within a hydrologically diverse Arctic landscape: 2. Modeled impacts of climate change, J. Geophys. Res. Biogeosciences, 120(7), 1388–1406, doi:10.1002/2014JG002889, 2015.

Grant, R. F., Mekonnen, Z. A., Riley, W. J., Wainwright, H. M., Graham, D. and Torn, M.

https://doi.org/10.5194/bg-2020-177
Preprint. Discussion started: 3 July 2020

Biogeosciences Discussions

S.: Mathematical Modelling of Arctic Polygonal Tundra with Ecosys: 1. Microtopography Determines How Active Layer Depths Respond to Changes in Temperature and Precipitation, J. Geophys. Res. Biogeosciences, 122(12), 3161–3173, doi:10.1002/2017JG004035, 2017a.

Grant, R. F., Mekonnen, Z. A., Riley, W. J., Arora, B. and Torn, M. S.: Mathematical Modelling of Arctic Polygonal Tundra with Ecosys: 2. Microtopography Determines How CO2 and CH4 Exchange Responds to Changes in Temperature and Precipitation, J. Geophys. Res. Biogeosciences, 122(12), 3174–3187, doi:10.1002/2017JG004037, 2017b.

Grant, R. F., Mekonnen, Z. A., Riley, W. J., Arora, B. and Torn, M. S.: Modelling climate change impacts on an Arctic polygonal tundra. Part 2: Changes in $CO_2$ and $CH_4$ exchange depend on rates of permafrost thaw as affected by changes in vegetation and drainage, J. Geophys. Res. Biogeosciences, 2018JG004645, doi:10.1029/2018JG004645, 2019.

Hemes, K. S., Chamberlain, S. D., Eichelmann, E., Knox, S. H. and Baldocchi, D. D.: A Biogeochemical Compromise: The High Methane Cost of Sequestering Carbon in Restored Wetlands, Geophys. Res. Lett., 45(12), 6081–6091, doi:10.1029/2018GL077747, 2018.

Hinkel, K. M., Frohn, R. C., Nelson, F. E., Eisner, W. R. and Beck, R. A.: Morphometric and spatial analysis of thaw lakes and drained thaw lake basins in the western Arctic Coastal Plain, Alaska, Permafr. Periglac. Process., doi:10.1002/ppp.532, 2005.

Hodgkins, S. B., Tfaily, M. M., McCalley, C. K., Logan, T. A., Crill, P. M., Saleska, S. R., Rich, V. I. and Chanton, J. P.: Changes in peat chemistry associated with permafrost

https://doi.org/10.5194/bg-2020-177
Preprint. Discussion started: 3 July 2020



thaw increase greenhouse gas production, Proc. Natl. Acad. Sci., doi:10.1073/pnas.1314641111, 2014.

Iwata, H., Harazono, Y., Ueyama, M., Sakabe, A., Nagano, H., Kosugi, Y., Takahashi, K. and Kim, Y.: Methane exchange in a poorly-drained black spruce forest over permafrost observed using the eddy covariance technique, Agric. For. Meteorol., 214–215, 157–168, doi:10.1016/j.agrformet.2015.08.252, 2015.

Kirschke, S., Bousquet, P., Ciais, P., Saunois, M., Canadell, J. G., Dlugokencky, E. J., Bergamaschi, P., Bergmann, D., Blake, D. R., Bruhwiler, L., Cameron-Smith, P., Castaldi, S., Chevallier, F., Feng, L., Fraser, A., Heimann, M., Hodson, E. L., Houweling, S., Josse, B., Fraser, P. J., Krummel, P. B., Lamarque, J.-F., Langenfelds, R. L., Le Quéré, C., Naik, V., O'Doherty, S., Palmer, P. I., Pison, I., Plummer, D., Poulter, B., Prinn, R. G., Rigby, M., Ringeval, B., Santini, M., Schmidt, M., Shindell, D. T., Simpson, I. J., Spahni, R., Steele, L. P., Strode, S. A., Sudo, K., Szopa, S., van der Werf, G. R., Voulgarakis, A., van Weele, M., Weiss, R. F., Williams, J. E. and Zeng, G.: Three decades of global methane sources and sinks, Nat. Geosci., 6(10), 813–823, doi:10.1038/ngeo1955, 2013.

Knoblauch, C., Beer, C., Liebner, S., Grigoriev, M. N. and Pfeiffer, E. M.: Methane production as key to the greenhouse gas budget of thawing permafrost, Nat. Clim. Chang., 1–4, doi:10.1038/s41558-018-0095-z, 2018.

Malmer, N., Johansson, T., Olsrud, M. and Christensen, T. R.: Vegetation, climatic changes and net carbon sequestration in a North-Scandinavian subarctic mire over 30 years, Glob. Chang. Biol., doi:10.1111/j.1365-2486.2005.01042.x, 2005.

McCalley, C. K., Woodcroft, B. J., Hodgkins, S. B., Wehr, R. A., Kim, E.-H., Mondav, R.,

https://doi.org/10.5194/bg-2020-177
Preprint. Discussion started: 3 July 2020


Biogeosciences Discussions

Crill, P. M., Chanton, J. P., Rich, V. I., Tyson, G. W. and Saleska, S. R.: Methane dynamics regulated by microbial community response to permafrost thaw, Nature, 514(7523), 478–481, doi:10.1038/nature13798, 2014.

Melton, J. R., Wania, R., Hodson, E. L., Poulter, B., Ringeval, B., Spahni, R., Bohn, T., Avis, C. A., Beerling, D. J., Chen, G., Eliseev, A. V., Denisov, S. N., Hopcroft, P. O., Lettenmaier, D. P., Riley, W. J., Singarayer, J. S., Subin, Z. M., Tian, H., Zürcher, S., Brovkin, V., van Bodegom, P. M., Kleinen, T., Yu, Z. C. and Kaplan, J. O.: Present state of global wetland extent and wetland methane modelling: conclusions from a model inter-comparison project (WETCHIMP), Biogeosciences, 10(2), 753–788, doi:10.5194/bg-10-753-2013, 2013.

Metcalfe, D. B., Hermans, T. D. G., Ahlstrand, J., Becker, M., Berggren, M., Björk, R. G., Björkman, M. P., Blok, D., Chaudhary, N., Chisholm, C., Classen, A. T., Hasselquist, N. J., Jonsson, M., Kristensen, J. A., Kumordzi, B. B., Lee, H., Mayor, J. R., Prevéy, J., Pantazatou, K., Rousk, J., Sponseller, R. A., Sundqvist, M. K., Tang, J., Uddling, J., Wallin, G., Zhang, W., Ahlström, A., Tenenbaum, D. E. and Abdi, A. M.: Patchy field sampling biases understanding of climate change impacts across the Arctic, Nat. Ecol. Evol., 2(9), 1443–1448, doi:10.1038/s41559-018-0612-5, 2018.

Myhre, G., D., Shindell, F.-M., Bréon, Collins, W., Fuglestvedt, J., Huang, J., Koch, D., Lamarque, J.-F., D. Lee, Mendoza, B., Nakajima, T., A. Robock, G. Stephens, Takemura, T. and Zhang, H.: Anthropogenic and Natural Radiative Forcing, in Climate Change 2013 - The Physical Science Basis, vol. 23, edited by Intergovernmental Panel on Climate Change, pp. 659–740, Cambridge University Press, Cambridge., 2013.

Neubauer, S. C. and Megonigal, J. P.: Moving Beyond Global Warming Potentials to

https://doi.org/10.5194/bg-2020-177
Preprint. Discussion started: 3 July 2020



Quantify the Climatic Role of Ecosystems, Ecosystems, 18(6), 1000–1013, doi:10.1007/s10021-015-9879-4, 2015.

Olefeldt, D. and Roulet, N. T.: Effects of permafrost and hydrology on the composition and transport of dissolved organic carbon in a subarctic peatland complex, J. Geophys. Res. Biogeosciences, 117(1), 1–15, doi:10.1029/2011JG001819, 2012.

Olefeldt, D., Turetsky, M. R., Crill, P. M. and Mcguire, A. D.: Environmental and physical controls on northern terrestrial methane emissions across permafrost zones, Glob. Chang. Biol., 19(2), 589–603, doi:10.1111/gcb.12071, 2013.

Poulter, B., Bousquet, P., Canadell, J. G., Ciais, P., Peregon, A., Saunois, M., Arora, V. K., Beerling, D. J., Brovkin, V., Jones, C. D., Joos, F., Gedney, N., Ito, A., Kleinen, T., Koven, C. D., McDonald, K., Melton, J. R., Peng, C., Peng, S., Prigent, C., Schroeder, R., Riley, W. J., Saito, M., Spahni, R., Tian, H., Taylor, L., Viovy, N., Wilton, D., Wiltshire, A., Xu, X., Zhang, B., Zhang, Z. and Zhu, Q.: Global wetland contribution to 2000–2012 atmospheric methane growth rate dynamics, Environ. Res. Lett., 12(9), 094013, doi:10.1088/1748-9326/aa8391, 2017.

Rinne, J., Tuittila, E. S., Peltola, O., Li, X., Raivonen, M., Alekseychik, P., Haapanala, S., Pihlatie, M., Aurela, M., Mammarella, I. and Vesala, T.: Temporal Variation of Ecosystem Scale Methane Emission From a Boreal Fen in Relation to Temperature, Water Table Position, and Carbon Dioxide Fluxes, Global Biogeochem. Cycles, 32(7), 1087–1106, doi:10.1029/2017GB005747, 2018.

Rydén, B. E. and Kostov, L.: Thawing and Freezing in Tundra Soils, Ecol. Bull., (30), 251–281 [online] Available from: http://www.jstor.org/stable/20112776, 1980.

https://doi.org/10.5194/bg-2020-177
Preprint. Discussion started: 3 July 2020


Saunois, M., Bousquet, P., Poulter, B., Peregon, A., Ciais, P., Canadell, J. G., Dlugokencky, E. J., Etiope, G., Bastviken, D., Houweling, S., Janssens-Maenhout, G., Tubiello, F. N., Castaldi, S., Jackson, R. B., Alexe, M., Arora, V. K., Beerling, D. J., Bergamaschi, P., Blake, D. R., Brailsford, G., Brovkin, V., Bruhwiler, L., Crevoisier, C., Crill, P., Covey, K., Curry, C., Frankenberg, C., Gedney, N., Höglund-Isaksson, L., Ishizawa, M., Ito, A., Joos, F., Kim, H. S., Kleinen, T., Krummel, P., Lamarque, J. F., Langenfelds, R., Locatelli, R., Machida, T., Maksyutov, S., McDonald, K. C., Marshall, J., Melton, J. R., Morino, I., Naik, V., O'Doherty, S., Parmentier, F. J. W., Patra, P. K., Peng, C., Peng, S., Peters, G. P., Pison, I., Prigent, C., Prinn, R., Ramonet, M., Riley, W. J., Saito, M., Santini, M., Schroeder, R., Simpson, I. J., Spahni, R., Steele, P., Takizawa, A., Thornton, B. F., Tian, H., Tohjima, Y., Viovy, N., Voulgarakis, A., Van Weele, M., Van Der Werf, G. R., Weiss, R., Wiedinmyer, C., Wilton, D. J., Wiltshire, A., Worthy, D., Wunch, D., Xu, X., Yoshida, Y., Zhang, B., Zhang, Z. and Zhu, Q.: The global methane budget 2000-2012, Earth Syst. Sci. Data, 8(2), 697–751, doi:10.5194/essd-8-697-2016, 2016.

Saunois, M., Bousquet, P., Poulter, B., Peregon, A., Ciais, P., Canadell, J. G., Dlugokencky, E. J., Etiope, G., Bastviken, D., Houweling, S., Janssens-Maenhout, G., Tubiello, F. N., Castaldi, S., Jackson, R. B., Alexe, M., Arora, V. K., Beerling, D. J., Bergamaschi, P., Blake, D. R., Brailsford, G., Bruhwiler, L., Crevoisier, C., Crill, P., Covey, K., Frankenberg, C., Gedney, N., Höglund-Isaksson, L., Ishizawa, M., Ito, A., Joos, F., Kim, H. S., Kleinen, T., Krummel, P., Lamarque, J. F., Langenfelds, R., Locatelli, R., Machida, T., Maksyutov, S., Melton, J. R., Morino, I., Naik, V., O'Doherty, S., Parmentier, F. J. W., Patra, P. K., Peng, C., Peng, S., Peters, G. P., Pison, I., Prinn, R.,

https://doi.org/10.5194/bg-2020-177
Preprint. Discussion started: 3 July 2020



Ramonet, M., Riley, W. J., Saito, M., Santini, M., Schroeder, R., Simpson, I. J., Spahni, R., Takizawa, A., Thornton, B. F., Tian, H., Tohjima, Y., Viovy, N., Voulgarakis, A., Weiss, R., Wilton, D. J., Wiltshire, A., Worthy, D., Wunch, D., Xu, X., Yoshida, Y., Zhang, B., Zhang, Z. and Zhu, Q.: Variability and quasi-decadal changes in the methane budget over the period 2000-2012, Atmos. Chem. Phys., 17(18), 11135–11161, doi:10.5194/acp-17-11135-2017, 2017.

Schuur, E. A. G., McGuire, A. D., Schädel, C., Grosse, G., Harden, J. W., Hayes, D. J., Hugelius, G., Koven, C. D., Kuhry, P., Lawrence, D. M., Natali, S. M., Olefeldt, D., Romanovsky, V. E., Schaefer, K., Turetsky, M. R., Treat, C. C. and Vonk, J. E.: Climate change and the permafrost carbon feedback, Nature, 520(7546), 171–179, doi:10.1038/nature14338, 2015.

Shiklomanov, N. I., Streletskiy, D. A., Nelson, F. E., Hollister, R. D., Romanovsky, V. E., Tweedie, C. E., Bockheim, J. G. and Brown, J.: Decadal variations of active-layer thickness in moisture-controlled landscapes, Barrow, Alaska, J. Geophys. Res. Biogeosciences, doi:10.1029/2009JG001248, 2010.

Tang, J. and Riley, W. J.: Weaker soil carbon-climate feedbacks resulting from microbial and abiotic interactions, Nat. Clim. Chang., advance on(January), doi:10.1038/nclimate2438, 2014.

Updegraff, K., Bridgham, S. D., Pastor, J. and Weishampel, P.: Hysteresis in the temperature response of carbon dioxide and methane production in peat soils, Biogeochemistry, 43(3), 253–272, doi:10.1023/A:1006097808262, 1998.

Wainwright, H. M., Dafflon, B., Smith, L. J., Hahn, M. S., Curtis, J. B., Wu, Y., Ulrich, C., Peterson, J. E., Torn, M. S. and Hubbard, S. S.: Identifying multiscale zonation and

https://doi.org/10.5194/bg-2020-177
Preprint. Discussion started: 3 July 2020




assessing the relative importance of polygon geomorphology on carbon fluxes in an Arctic tundra ecosystem, J. Geophys. Res. Biogeosciences, doi:10.1002/2014JG002799, 2015.

Wania, R., Melton, J. R., Hodson, E. L., Poulter, B., Ringeval, B., Spahni, R., Bohn, T., Avis, C. A., Chen, G., Eliseev, A. V., Hopcroft, P. O., Riley, W. J., Subin, Z. M., Tian, H., Van Bodegom, P. M., Kleinen, T., Yu, Z. C., Singarayer, J. S., Zürcher, S., Lettenmaier, D. P., Beerling, D. J., Denisov, S. N., Prigent, C., Papa, F. and Kaplan, J. O.: Present state of global wetland extent and wetland methane modelling: Methodology of a model inter-comparison project (WETCHIMP), Geosci. Model Dev., 6(3), 617–641, doi:10.5194/gmd-6-617-2013, 2013.

Wik, M., Varner, R. K., Anthony, K. W., MacIntyre, S. and Bastviken, D.: Climate-sensitive northern lakes and ponds are critical components of methane release, Nat. Geosci., 9(2), 99–105, doi:10.1038/ngeo2578, 2016.

Xu, X., Yuan, F., Hanson, P. J., Wullschleger, S. D., Thornton, P. E., Riley, W. J., Song, X., Graham, D. E., Song, C. and Tian, H.: Reviews and syntheses: Four decades of modeling methane cycling in terrestrial ecosystems, Biogeosciences, 13(12), 3735–3755, doi:10.5194/bg-13-3735-2016, 2016.

Yvon-Durocher, G., Allen, A. P., Bastviken, D., Conrad, R., Gudasz, C., St-Pierre, A., Thanh-Duc, N. and Del Giorgio, P. A.: Methane fluxes show consistent temperature dependence across microbial to ecosystem scales, Nature, 507(7493), 488–491, doi:10.1038/nature13164, 2014.

Zona, D., Gioli, B., Commane, R., Lindaas, J., Wofsy, S. C. and Miller, C. E.: Cold season emissions dominate the Arctic tundra methane budget, Proc. Natl. Acad. Sci., 113(1),

https://doi.org/10.5194/bg-2020-177
Preprint. Discussion started: 3 July 2020



40–45, doi:10.1073/pnas.1516017113, 2016.

https://doi.org/10.5194/bg-2020-177
Preprint. Discussion started: 3 July 2020


Biogeosciences
Discussions

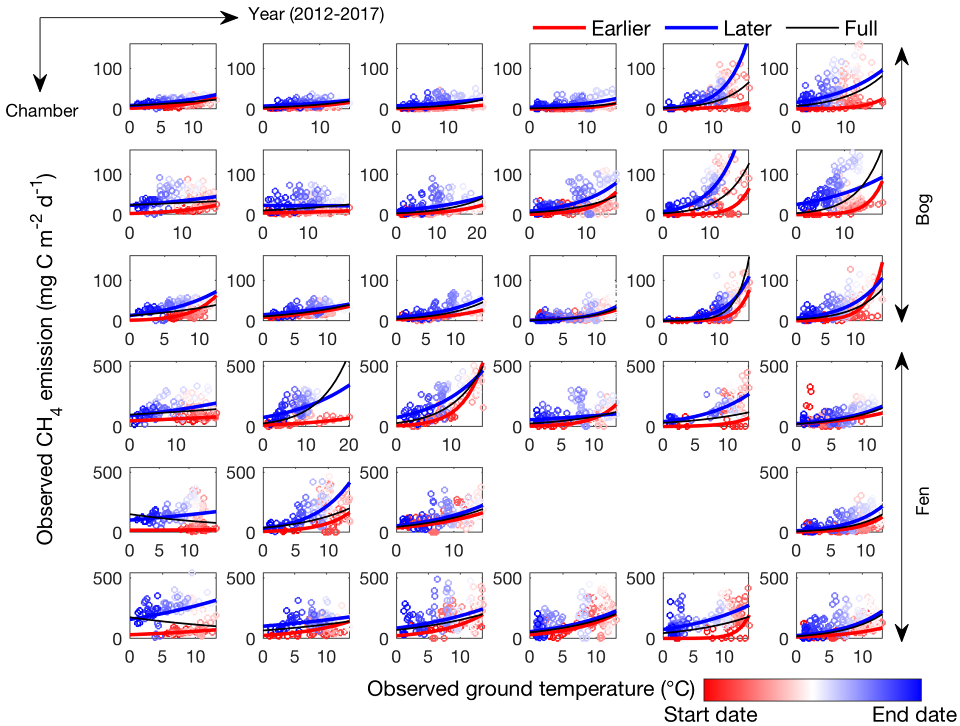


Figure 1. $CH_4$ emissions are hysteretic to ground surface temperature measured in individual automated chambers in the Stordalen Mire bog (top three panels) and fen (bottom three panels) sites from 2012 to 2017 thawed seasons (left to right). Open circles and lines represent the daily data points and the fitted apparent $CH_4$ emission temperature dependence, respectively. The earlier, later, and full-season periods are colored in red, blue, and black, respectively. Earlier and later periods are defined as the time before and after the seasonal maximum ground surface temperature. Start date and end dates represent the beginning and ending of a thawed season defined as the period when daily ground surface temperature is above 1 ˚C, respectively.

https://doi.org/10.5194/bg-2020-177
Preprint. Discussion started: 3 July 2020


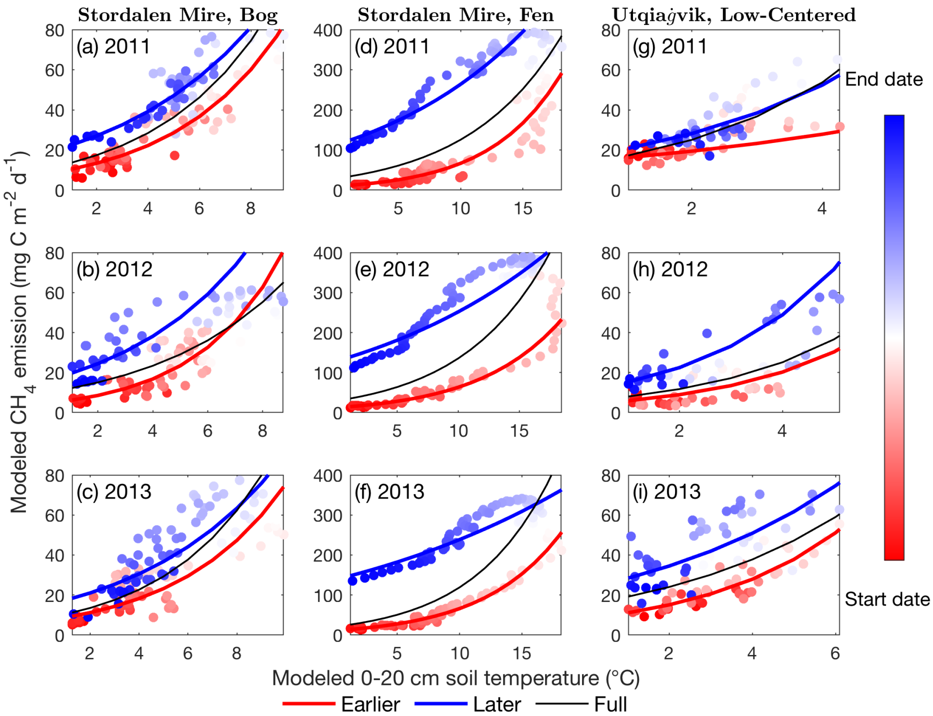


Figure 2. $CH_4$ emissions are hysteretic to soil temperature modeled in the Stordalen Mire bog (a to c) and fen (d to f) and the Utqiaġvik low-centered polygon (g to i) from 2011 to 2013 thawed seasons. Dots and lines represent the daily data points and the fitted apparent temperature dependence, respectively. Earlier, later, and full-season periods are colored in red, blue, and black, respectively. Earlier and later periods are defined as the time before and after the seasonal maximum 0-20 cm soil temperature. Start date and end dates represent the beginning and ending of a thawed season defined as the period when daily 0-20 cm soil temperature is above 1 ˚C, respectively.

https://doi.org/10.5194/bg-2020-177
Preprint. Discussion started: 3 July 2020



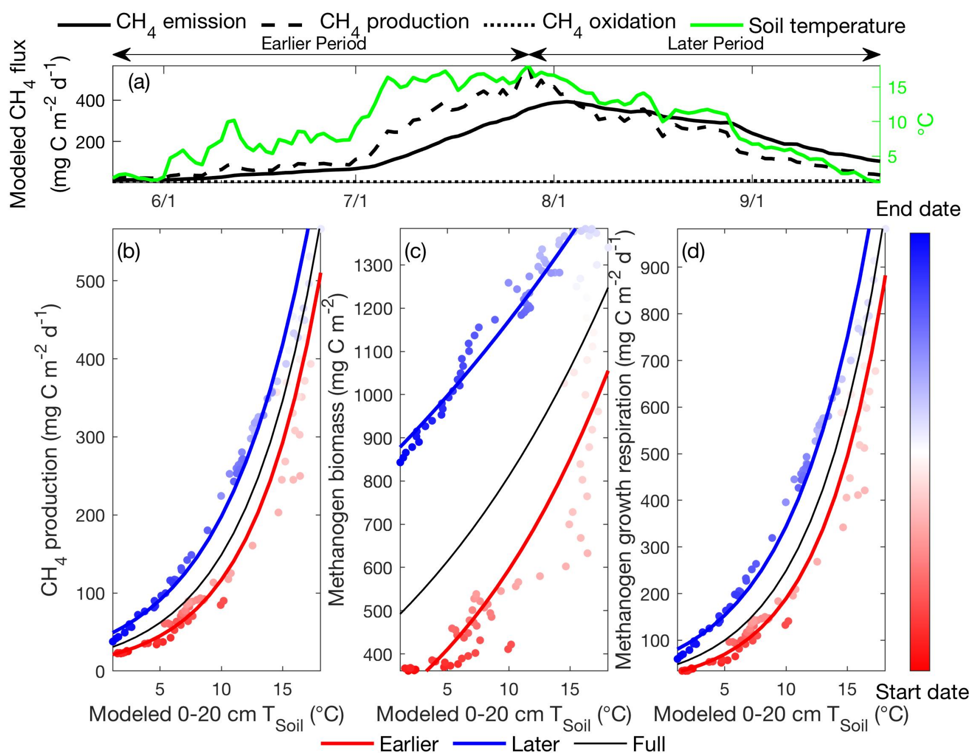


Figure 3. Intra-seasonal variations in apparent $CH_4$ production temperature dependence result from asymmetric microbial biomass and activity modeled between the earlier and later periods. Daily $CH_4$ emissions, $CH_4$ production, $CH_4$ oxidation, and 0-20 cm soil temperature modeled in the Stordalen Mire fen during the 2011 thawed season (a). The corresponding apparent temperature dependence of the modeled $CH_4$ production (b), methanogen biomass (c), and methanogen growth respiration (d) during the 2011 thawed season. Earlier, later, and full-season periods are colored in red, blue, and black, respectively. Earlier and later periods are defined as the time before and after the seasonal maximum 0-20 cm soil temperature. Start date and end dates represent the beginning and ending of a thawed season defined as the period when daily 0-20 cm soil temperature is above 1 ˚C, respectively.

https://doi.org/10.5194/bg-2020-177
Preprint. Discussion started: 3 July 2020




674 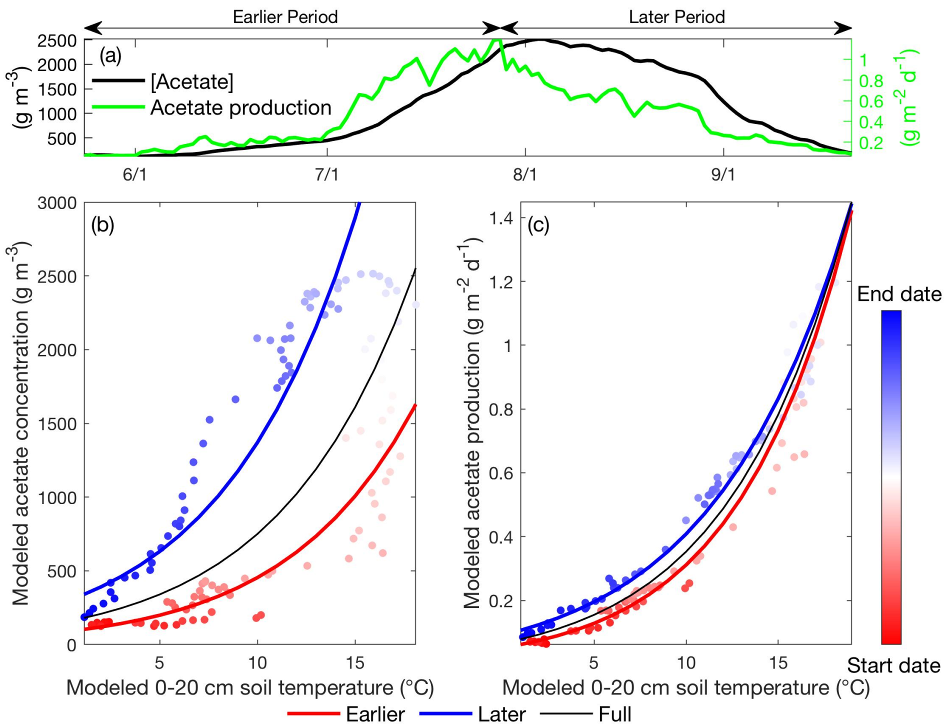


675 Figure 4. Daily acetate concentration and acetate production modeled in the Stordalen
676 Mire fen during the 2011 thawed season (a). The corresponding apparent temperature
677 dependence of the modeled acetate concentration (b) and acetate production (c) during
678 the 2011 thawed season. Dots and lines represent the daily data points and the fitted
679 apparent temperature dependence, respectively. The earlier, later, and full-season periods
680 are colored in red, blue, and black, respectively. Earlier and later periods are defined as
681 the time before and after the seasonal maximum soil temperature (0-20 cm). Start date
682 and end dates represent the beginning and ending of a thawed season defined as the
683 period when daily 0-20 cm soil temperature is above 1 °C, respectively.

684

https://doi.org/10.5194/bg-2020-177
Preprint. Discussion started: 3 July 2020

Biogeosciences
Discussions
Open Access

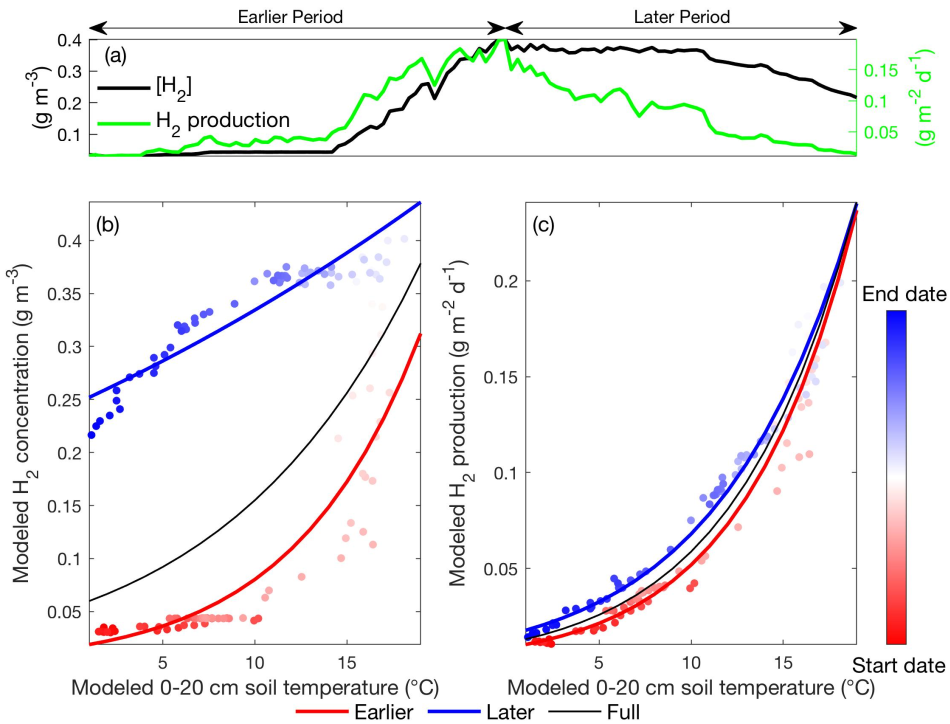


Figure 5. Daily hydrogen concentration and hydrogen production modeled in the Stordalen Mire fen during the 2011 thawed season (a). The corresponding apparent temperature dependence of the modeled hydrogen concentration (b) and hydrogen production (c) during the 2011 thawed season. Dots and lines represent the daily data points and the fitted apparent temperature dependence, respectively. The earlier, later, and full-season periods are colored in red, blue, and black, respectively. Earlier and later periods are defined as the time before and after the seasonal maximum soil temperature (0-20 cm). Start date and end dates represent the beginning and ending of a thawed season defined as the period when daily 0-20 cm soil temperature is above 1 ˚C, respectively.

https://doi.org/10.5194/bg-2020-177
Preprint. Discussion started: 3 July 2020




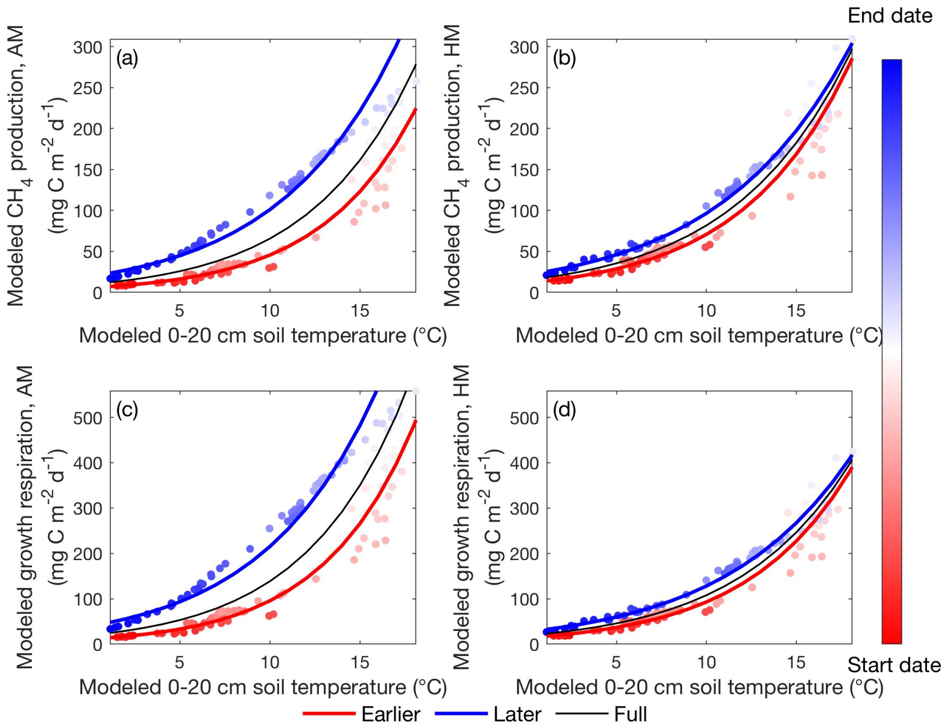


Figure 6. Apparent temperature dependence of daily $CH_4$ production for acetoclastic (a) and hydrogenotrophic (b) methanogenesis, and daily growth respiration for acetoclastic (c) and hydrogenotrophic (d) methanogens modeled in the Stordalen Mire fen during the 2011 thawed season. Dots and lines represent the daily data points and the fitted apparent temperature dependence, respectively. The earlier, later, and full-season periods are colored in red, blue, and black, respectively. Earlier and later periods are defined as the time before and after the seasonal maximum soil temperature (0-20 cm). Start date and end dates represent the beginning and ending of a thawed season defined as the period when daily 0-20 cm soil temperature is above 1 ˚C, respectively.

https://doi.org/10.5194/bg-2020-177
Preprint. Discussion started: 3 July 2020


Biogeosciences
Discussions

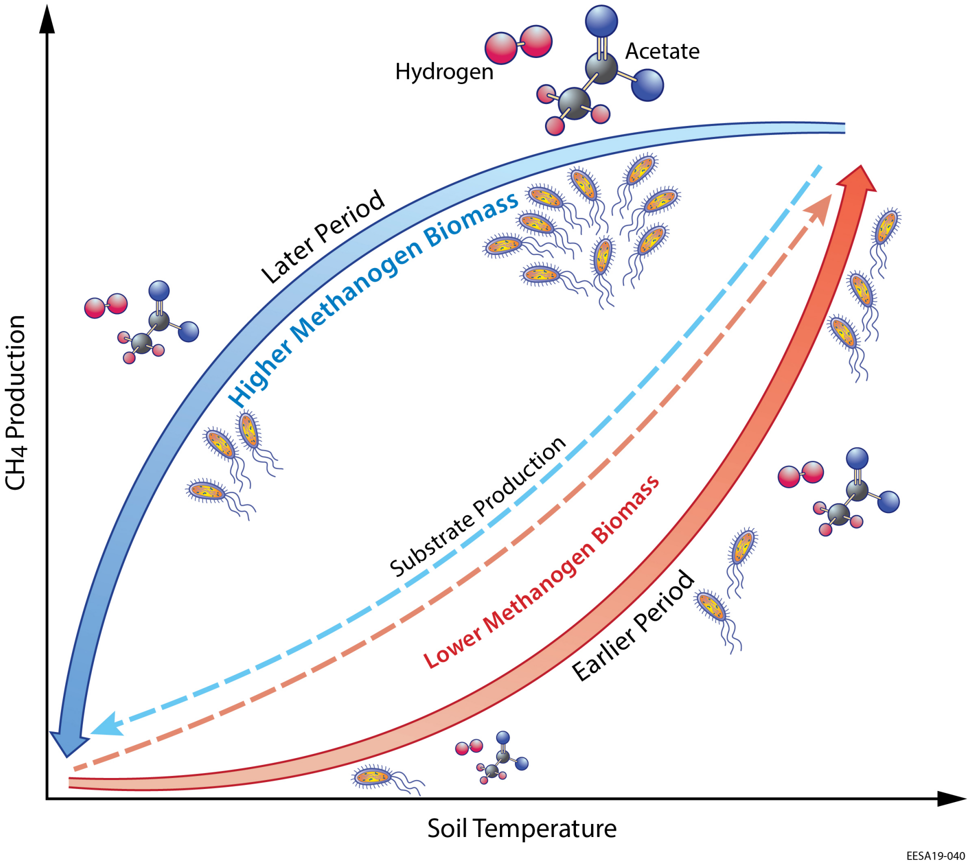


707

708 Figure 7. Schematic of the microbial substrate-mediated $CH_4$ production hysteresis

709 proposed in this study. Higher substrate (i.e., acetate and hydrogen) availability

710 stimulates higher methanogen biomass during the later period, which leads to intra-

711 seasonal differences in $CH_4$ production between the earlier and later periods.

712

https://doi.org/10.5194/bg-2020-177
Preprint. Discussion started: 3 July 2020


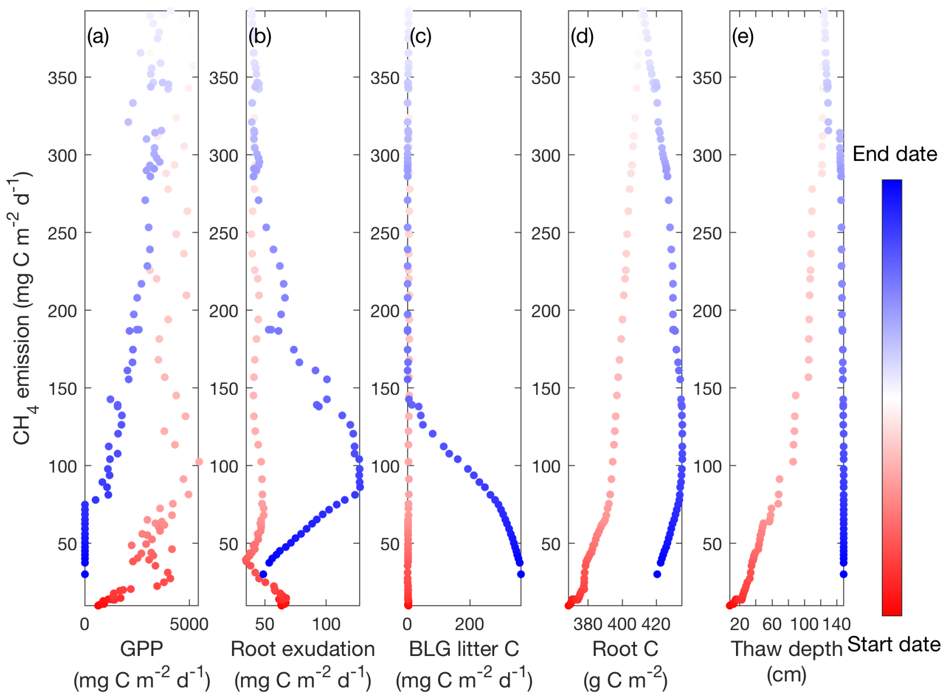


Figure 8. Daily $CH_4$ emissions have hysteretic responses to gross primary productivity (a), carbon released from root exudation (b), carbon released from belowground litter decomposition (c), the amount of root biomass for sedges (d), and thaw depth (e) modeled in the Stordalen Mire fen during the 2011 thawed season. Dots and lines represent the daily data points and the fitted apparent temperature dependence, respectively. Start date and end dates represent the beginning and ending of a thawed season defined as the period when daily 0-20 cm soil temperature is above 1 ˚C, respectively.

https://doi.org/10.5194/bg-2020-177
Preprint. Discussion started: 3 July 2020




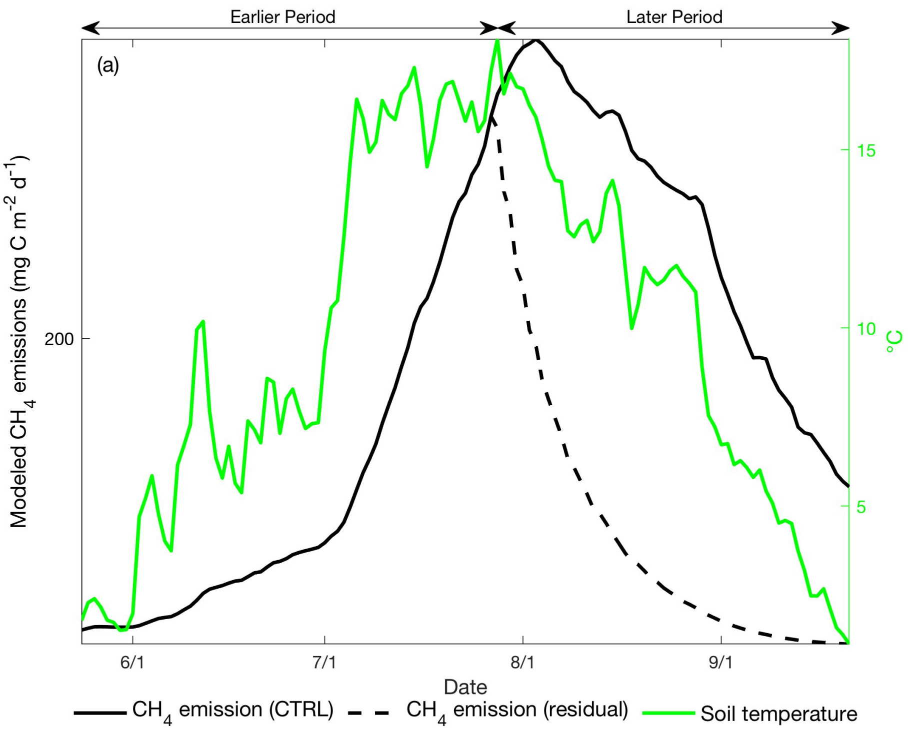


Figure 9. Daily $CH_4$ emissions (black line, left axis) and 0-20 cm mean soil temperature (green line, right axis) modeled in the Stordalen Mire fen during the 2011 thawed season. Black solid and dashed lines represent the modeled $CH_4$ emissions with and without $CH_4$ production during the later period, respectively. Earlier and later periods are defined as the time before and after the seasonal maximum soil temperature (0-20 cm).